Nanoparticle dynamics in hydrogel networks with controlled defects

Katie A. Rose, Emanuele Marino, Christopher S. O'Bryan, Christopher B. Murray, Daeyeon Lee, Russell J. Composto

Supplemental Information

I Nanoparticle characterization

Fluorescent polystyrene (PS) was purchased from Bangs Labs. Scanning electron microscopy was used to visualize the PS nanoparticles (Fig. S1). Prior to imaging, the samples were sputtered with 4 nm of iridium to prevent charging. To determine the hydrodynamic diameter, d_h of the polystyrene particles in water, dynamic light scattering was used (Delsa Nano-C, Beckman Coulter). The differential intensity profile was fit to a Gaussian with the center indicating an average r_h of 47.1 nm (Fig. S2).

Transmission electron microscopy (TEM) was used to determine the size of the core/shell of each of the CdSe/CdS QD set and found to have a diameter of 9.6 nm (QD1) and 5 nm (QD2) (Fig. S1). The larger set of QDs (CdSe/CdS = 9.6 nm) were received in toluene, functionalized with oleic acid. The smaller set of QDs (CdSe/CdS = 5 nm), were similarly functionalized with oleic acid, but received in hexane. Prior to additional modification, the 9.6 nm CdSe/CdS nanoparticles were dried and re-dispersed in toluene.

Post 5 kg/mol thiol-poly(ethylene glycol) (PEG) functionalization, the hydrodynamic size of each QD was calculated by measuring the ensemble mean squared displacement (MSD) via particle tracking in glycerol-water (70, 80, 90 v%) solutions of known viscosity to determine the diffusion coefficient from the following equation,

$$MSD = 2nD\tau \tag{1}$$

where n is a dimensionality factor, D is the diffusion coefficient and τ is the lag time. The Stokes-Einstein equation can then be used to calculate the hydrodynamic diameter, d_h.

$$D = \frac{k_b T}{3\pi\eta d_h} \tag{2}$$

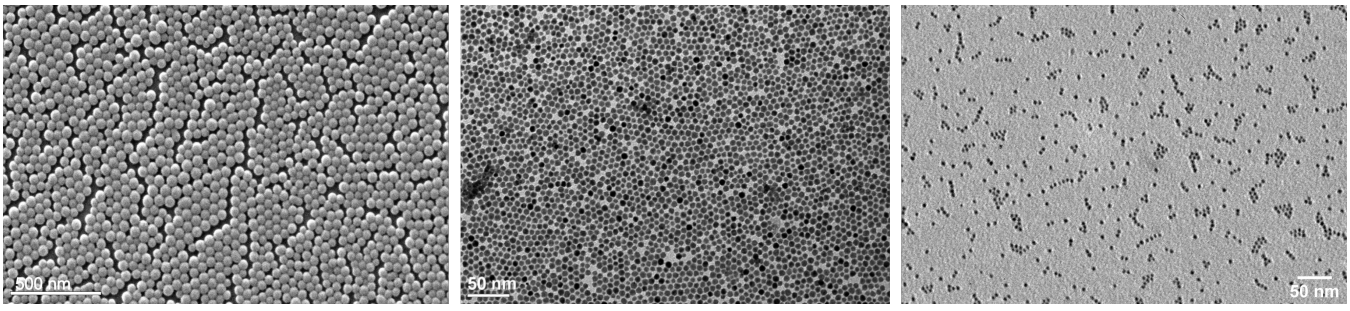

Figure 1: Scanning electron microscopy (SEM) of the fluorescent polystyrene nanoparticles (left) and transmission electron microscopy (TEM) of the oleic acid functionalized quantum dot nanoparticles, CdSe/CdS 9.6 nm (middle) and 5.0 nm (right).

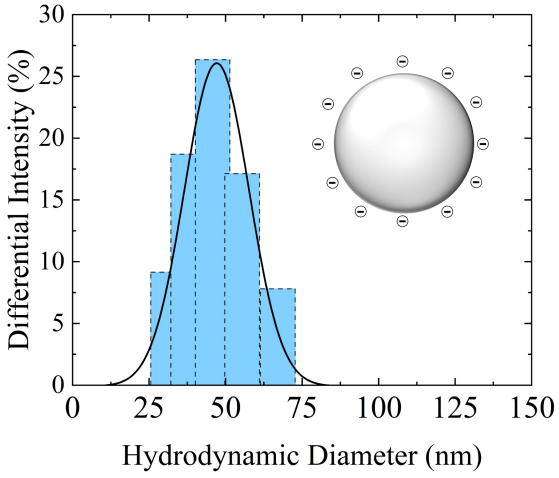

Figure 2: Dynamic light scattering (DLS) of fluorescent polystyrene particles.

where k_b is the Boltzmann's constant, T is the solution temperature, and η is the solution viscosity, known for glycerol-water solutions at a given volume % of glycerol. The hydrodynamic diameter was calculated to be $d_h = 15.1$ nm for the larger QDs ($d = 9.6$ nm, TEM) and $d_h = 9.6$ nm for the smaller QDs ($d = 5$ nm, TEM). Previous work has shown that a 5 kg/mol PEG functionalization results in ~ 5 nm of additional hydrodynamic diameter, which aligns well with this work.[1]

The van Hove distribution function, or the probability distribution of particle displacements, is plotted at $\tau = 0.3$ seconds for each of the QD probes in 90 v% glycerol-water solutions (Fig. S3). For a homogeneous probe diffusing in a homogeneous fluid (i.e. glycerol-water solutions) the probability distribution function can be fit by a Gaussian profile. For both QDs, the distribution is fit well by a Gaussian, indicating that the particles are relatively homogeneous after PEG-functionalization.

II Reaction-tuned hydrogel characterization

With the addition of defects, the dangling ends contain charged end groups at physiological pH. To determine if the electrostatic interactions between the charged carboxylic acid and amine end groups impacted nanoparticle dynamics, the dynamics of 47.1 nm PS particles were examined in degraded solutions of 1) TPEG-SG and 2) TPEG-SG and TPEG-A. Tetra-PEG macromers were degraded in buffer overnight to fully hydrolyze the NHS ester of the TPEG-SG. For the solution with both tetra-PEG macromers, the TPEG-SG and TPEG-A were then mixed with trace amounts of PS nanoparticles and allowed to mix overnight. Tilt tests indicated no gel had formed 12 hours after mixing. Figure S4 shows the van Hove distribution function of the PS nanoparticles in solutions of the degraded TPEG-SG and the degraded TPEG-SG mixed with TPEG-A. The displacements are well described by a Gaussian fit, with limited changes in displacements between both solutions.

While just the storage modulus, G', is shown in the main text for clarity, examples of the crossover of storage, G', and loss G'', moduli are included here for $t_{hyd} = 0$ and 15 minutes (Fig. S5). The crossover of G' and G'' is indicative of the formation of a percolated network throughout the solution, t_{gel}. As t_{hyd} increases, so does t_{gel} indicating that the reduction in the number of available crosslinking sites increases the time for a percolated network to form. t_{gel} ranges from 24 minutes at $t_{hyd} = 0$ minutes (the most homogeneous network) to 93.5 minutes at $t_{hyd} = 75$ minutes (the most defective network), an almost 4 times increase.

To calculate the swollen mesh size, ξ_s, swelling studies were conducted for $t_{hyd} = 0, 15, 30, 45, 60$ and 75 minutes (Fig. S6). The lowest degree of swelling occurs at $t_{hyd} = 0$ minutes, with the mass swelling ratio monotonically increasing with increasing t_{hyd}.

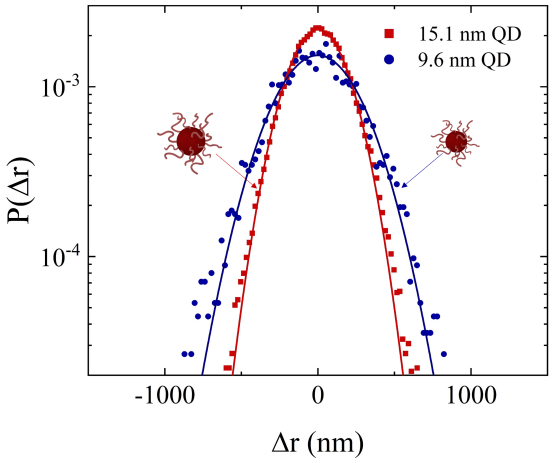

Figure 3: van Hove distribution function of PEG-functionalized CdSe/CdS quantum dots (QD) of two different sizes, hydrodynamic diameter 15.1 nm and 9.6 nm.

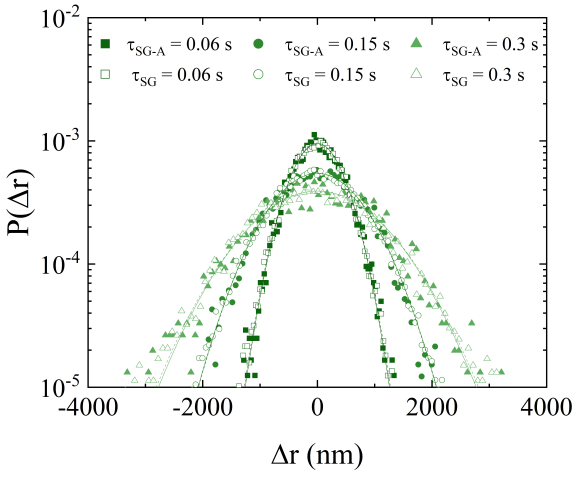

Figure 4: van Hove distribution function of 47.1 nm polystyrene nanoparticles in a degraded solution of 1) 40 mg/mL TPEG-SG (open points) and 2) 40 mg/mL TPEG-SG and TPEG-A (closed points) at $\tau = 0.06, 0.15$ and 0.3 seconds. Solid and dashed lines are Gaussian fits to the closed and open points, respectively.

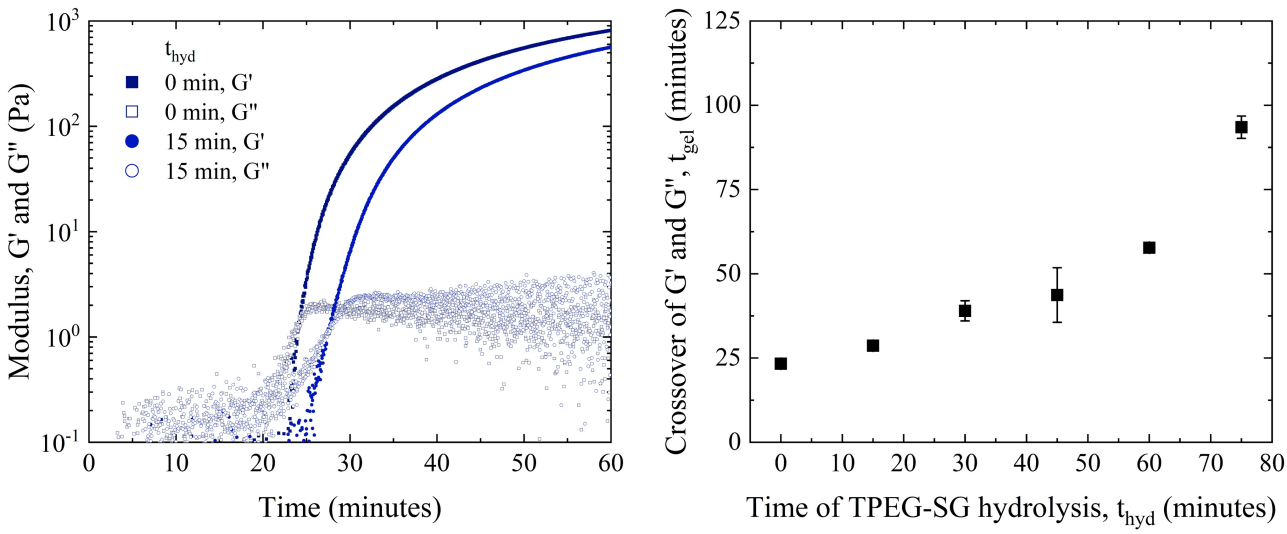

Figure 5: Time sweep over the gelation of the hydrogel tetra-PEG, focused on the crossover of G' (closed symbols) and G'' (open symbols) for $t_{hyd} = 0$ minutes (dark blue squares) and $t_{hyd} = 15$ minutes (light blue circles). Data is offset to account for the sample prep post mixing (left). t_{gel} as a function of t_{hyd} from $t_{hyd} = 0$ to 75 minutes (right). Error bars come from duplicate samples on separate days.

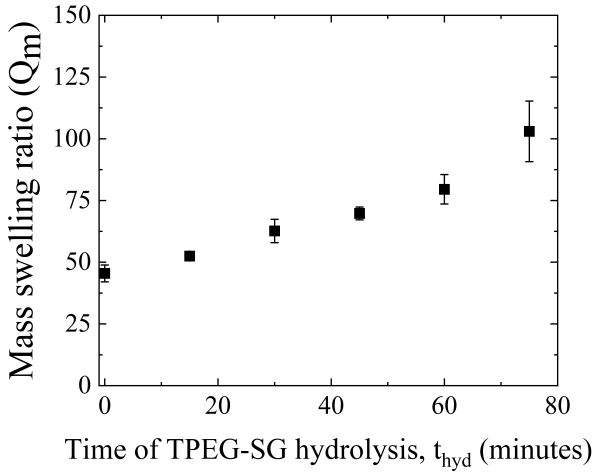

Figure 6: Mass swelling ratio, Q_m, of tetra-PEG hydrogels as a function of t_{hyd} between 0 and 75 minutes in 15 minute increments. Error bars come from duplicates over multiple days, representing at least five samples.

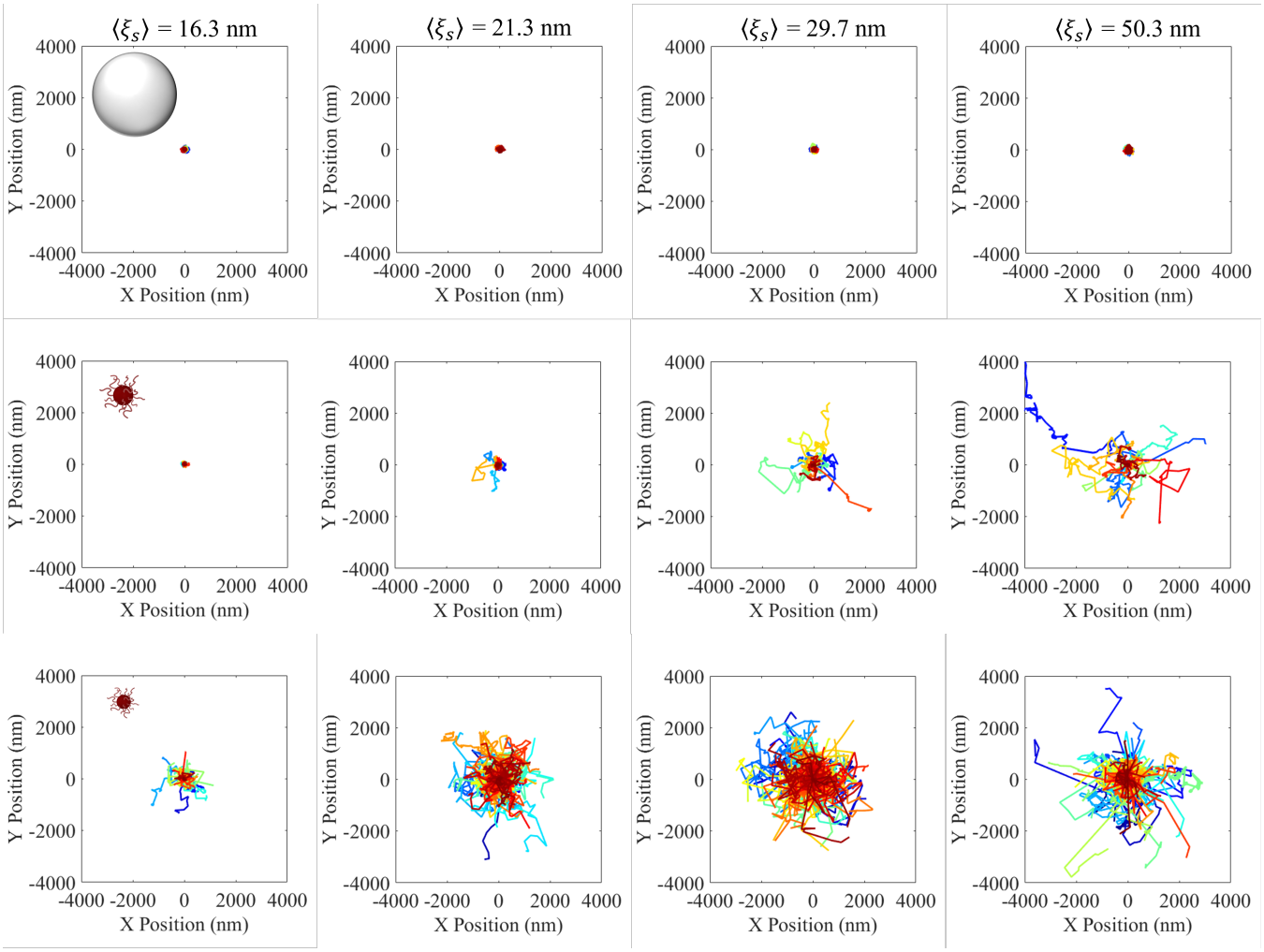

Figure 7: Particle trajectories of individual nanoparticles plotted in XY space of 47.1 nm polystyrene nanoparticles (top row), 15.1 nm PEG-functionalized quantum dots (QD) (middle row) and 9.6 nm PEG-functionalized QDs (bottom row) for $\langle \xi_s \rangle = 16.3, 21.3, 29.7$ and 50.3 nm. Trajectories are initialized at an origin of (0,0).

III Additional single particle tracking

The displacement of individual nanoparticles in the XY plane is shown in Figure S7 to emphasize the length scales of individual trajectories over the time of imaging. For the 47.1 nm polystyrene (PS) nanoparticle probes, there are limited changes as the network becomes more defective. Large displacements (above 2000 nm) are limited by the z-plane of imaging, though some particles still remain in the plane of imaging.

The van Hove distribution function at $\tau = 0.3$ seconds for the PS particles show small changes between $\langle \xi_s \rangle = 16.3$ nm and 50.3 nm (Fig. S8). These changes are minimal, the characteristic length from the decay of the exponential tail, λ, only increase from 14.0 nm to 16.8 nm from $\langle \xi_s \rangle = 16.3$ nm and 50.3. The small increase in placements does not appear to be due to an increase in mobile particles as displacements do not increase with increasing τ (Fig. S8, inset), but may represent small changes in the cage size of the localized PS particles as defects increase.

Figure S9 shows the van Hove distribution function for the 9.6 nm QDs at $\tau = 0.15$ seconds. While there is a clear increase in displacements between $\langle \xi_s \rangle = 16.3$ and 21.3 nm, as indicated by the increase in λ from 106.1 nm to 260.2 nm, respectively, changes at $\langle \xi_s \rangle = 29.7$ and 50.3 nm are convoluted by fast moving particles that are unable to be tracked. Some of these fast moving particles can be seen in the early τ regions of the MSDs in the $\langle \xi_s \rangle = 50.3$ nm networks (Fig. 8, main text), though many more were unable to be tracked and therefore the MSDs and displacements in these systems are not representative of the overall dynamics in these systems. Due to this, the focus in the main text

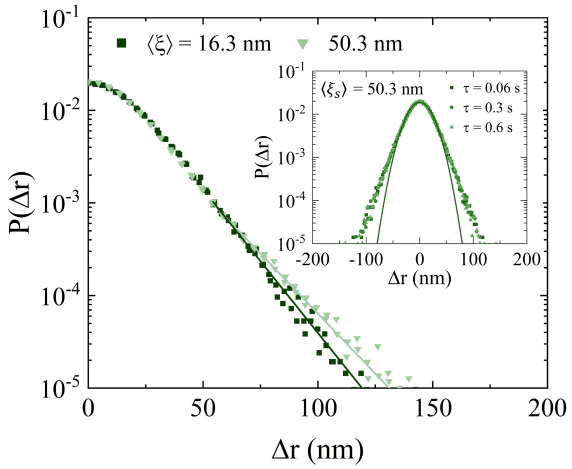

Figure 8: van Hove distribution function of 47.1 nm polystyrene nanoparticles in $\langle \xi_s \rangle = 16.3$ and 50.3 nm at $\tau = 0.3$ seconds. Inset shows the van Hove distribution function of 47.1 nm PS in $\langle \xi_s \rangle = 50.3$ nm at $\tau = 0.06, 0.3$ and 0.6 seconds. Line represents Gaussian fits to $\tau = 0.06$ seconds.

is on $\langle \xi_s \rangle = 16.3$ nm and 21.3 nm.

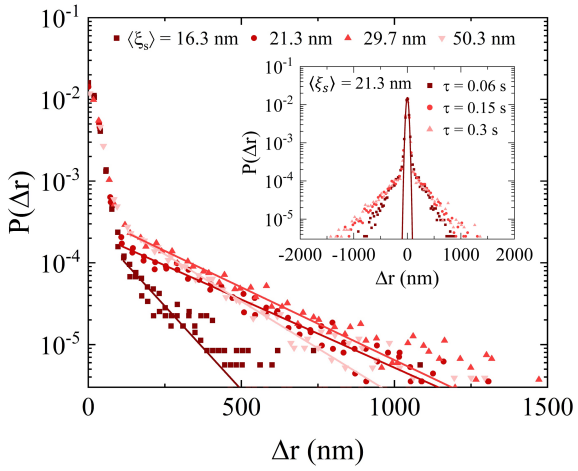

Figure 9: van Hove distribution function of 9.6 nm PEG-functionalized quantum dot (QD) nanoparticles for $\langle\xi_s\rangle = 16.3, 21.3, 29.7$ and 50.3 nm at $\tau = 0.15$ seconds. Inset shows the van Hove distribution function at $\langle\xi_s\rangle = 21.3$ nm as a function of τ, at $\tau = 0.06, 0.15$ and 0.3 seconds. Line shows a Gaussian fit to $\tau = 0.06$ seconds.

References

[1] K. A. Rose, D. Lee and R. J. Composto, *Soft Matter*, 2021, **17**, 2765–2774.